International Journal of GEOMATE, Nov, 2022, Vol.23, Issue 99, pp.141-150
ISSN: 2186-2982 (P), 2186-2990 (O), Japan, DOI: https://doi.org/10.21660/2022.99.3470
Geotechnique, Construction Materials and Environment

LIQUEFACTION POTENTIAL OF LAYERED SOIL UNDER VERTICAL VIBRATION LOADS

Faris Waleed Jawad[1], *Madhat Shakir Al-Soud[2], Mustafa Musa Salih [3], Nadhir Al-ansari [4], and Huda M. Madhloom[5]

[1,2,5] College of Engineering, Mustansiriyah University, Iraq
[3]Reconstruction and Projects Department, University of Baghdad, Iraq
[4] Department of Civil Environmental and Natural Resources Engineering, Luleå University of Technology, Sweden
*Corresponding Author, Received: 01 Oct. 2022, Revised: 02 Nov. 2022, Accepted: 27 Nov. 2022

ABSTRACT: The risk of liquefaction phenomena increases during dynamic loading and can cause the shear failure of soil under foundations. Model tests for a small-scale model under vertical vibration loads are presented. The operating frequency was changed from 1000, 2500 to 3500 revolutions per minute and the amplitude of loading with time was applied as a sine wave. Several parameters were considered, such as the force-time history of the machine foundation, the final settlement of the foundation, the vertical stress inside the soil media, the excess pore water pressure and observed liquefaction phenomena. These observations were compared to the effect of the sub-base layer thickness under the footing and its ability to reduce the liquefaction phenomena. The results showed that the shape of the load–time history coincides with a sine wave and the increase in the operating frequency led to an increase in the measured vibration load. The settlement was observed to increase with increases in the operating frequency. The settlement depended on the state of the soil and the operating frequency applied. Increases in operating frequency of about 3 times led to an increase in the time interval of excess pore pressure and reached a maximum value. The phenomenon of liquefaction appeared clearly when sandy soil was in a loose state. When the soil changes to a medium state, the phenomena of liquefaction respond to the operating frequency more than the operating frequency in a loose state. No liquefaction occurs in a dense state. The use of a subbase layer more than 1.5 times the depth of the footing led to eliminating the liquefaction phenomena.

Keywords: Numerical analysis, Experimental works, Machine foundation, Operating frequency, Liquefaction.

1. INTRODUCTION

Liquefaction happens when the saturated soil strength and stiffness are reduced by mechanical loading. The water is filled between the soil particles and exerts pressure on the particles due to mechanical movements like an earthquake or heavy equipment. Therefore, heavy equipment and machines with high speed, operating conditions and loads require special types of foundations, which are called "Machine foundations". To define the strength and stiffness of liquefied soil, the degree of liquefaction as characterized by the excess pore water pressure plays an important role [1].

Das and Ramana [2] stated that the nature of load producing source determines the dynamic loading (any moving load) type in soil or the structure foundation. Dynamic loadings may fluctuate in their position, direction, or magnitude with time, for example, vehicle traffic and equipment. The intensity of these dynamic loads may reflect variations with the time of day. Adalier and Elgamal [3] found that the rate of pore pressure generation and the induced settlements under seismic load were increased with decreasing the relative density and the over-consolidation ratio of the liquefiable sand layer. Al-Azawi et al. [4] conducted a dynamic response of machine foundations subjected to vertical load. They discovered that the footing's depth has a great influence on the dynamic behavior. On the other side, the dynamic stiffness and damping coefficients were increased with increasing the embedment depth.

The shape of pressure distribution is one of the main parameters to study when addressing machine foundation. In that respect, Chandrakaran et al. [5] found that the shape of pressure distribution changed from a parabolic shape to a rigid one due to an increase in the mass ratio of the foundation of the machine. Jafarzadeh and Asadinik [6] investigated three foundation shapes, circular, square, and rectangular. The results showed that two resonance frequencies were observed in the test results. The first is due to the wave's reflection, while the second is due to the inertia and the natural frequency of the system. Vivek and Ghosh [7] used PLAXIS 2D to study the effect of the dynamic interaction of two closely distance-embedded strip footing under the impact of machine vibration. The results showed the

response of the adjoining passive structure is signed up to a spacing of 2B from the actually exciting structure. Al-Shammary [8] investigated the dynamic behavior of strip foundations lying on saturated sandy soil. It was found that the embedment depth has a beneficial effect on the reduction in dynamic response.

Swain and Ghosh [9] presented an experimental work on the dynamic interaction of closely spaced square footing under machine vibration. The transmission ratio, which reveals the influence of dynamic excitation of the active foundation on the passive one, was obtained for the interacting footings and plotted with regard to the frequency ratio. Keawsawasvong et al. [10] presented rocking vibrations of a rigid foundation sitting on a multi-layered poroelastic half-space. Comparisons between the current model and existing resolutions on rocking vibration of rigid foundations on elastic and poroelastic media were illustrated. Foundations with different forms and mud were shown to have different rocking compliance values. There was also an example of dynamic interaction with near-foundation spacing under rocking vibrations to demonstrate the applicability of this solution strategy. They found that when the dimension ratio of a foundation (L/B) is greater than eight, then a rigid rectangular foundation could be analyzed under plane strain conditions performed for rocking vibrations. Hassan and Salwan [11] studied the dynamic response of square footings under the effect of dynamic load. The study showed that when the spacing between footings increases, the amplitude of velocity, displacement, and acceleration for the second footing decreases.

Tileylioglu et al. [12] performed a study in Garner Valley, California, with a large-scale model. The outcomes display that the damping will increase forcedly with frequency. Besides, it is stronger in translation than in rocking and pretends contributions from each radiation and hysteretic source. Alzabeebee [13] studied the efficiency of using skirts as a method to minimize the settlement of a strip footing under machine vibration. He found that the skirt's effect in reducing the dynamic settlement was reduced by increasing the soil stiffness. The percentages of settlement decrease were between (2% - 70%) for loose sand, (1% - 68%) for medium sand, and (0.5% - 67%) for dense sand. Fattah et al. [14] analyzed a case of machine foundation resting on a saturated sandy soil using QUAKE/W computer program. They found that increasing loading amplitude and frequency tends to accelerate the liquefaction and deformation when the foundation is constructed over loose saturated sand. Moreover, liquefaction propagates to reach a point at a depth of five times the foundation width. Javdanian [15] studied the dynamic bearing capacity of adjacent shallow strip footings located on sandy soil. The outcomes show it is very important to take into consideration the interference influence in the assessment of the bearing capacity of shallow foundations subjected to cyclic loading like vibrating machines foundations.

Choudhury & Rao [16] studied three different kinds of failure surfaces that are assumed the embedment depth and ground inclinations. The obtained outcomes, which display the influence of parametric difference on seismal bearing capacity factors, have been studied. Bhatia [17] showed the permissible limits of amplitude for different machines for different frequencies and the frequency classified as low-speed machines (100-1500 rpm), medium-speed machines (1500-3000) rpm and high-speed machines (3000-10000) rpm and above. Fattah et al. [18] showed that the settlement of a square foundation in medium sand was affected by the embedment.

The reduction percentages of settlement ranged from 15.2 to 17.3 % at a load amplitude of (0.5) tonne, from 6.7 to 10.5 % at a load amplitude of 1 tonne, and from 9.3 to 10.9 % with increasing applied load to 2 tonnes. At dense state sand, the reduction percentages in settlement value ranged from 25.2 to 42.5 % at load amplitude (0.5 tonnes), from 9.7 to 29.1 % at load amplitude of 1 tonne, and from 12.6 to 23.18 % at the load amplitude is 2 tonne. Fattah et al. [19] revealed that increasing the value of loading amplitude and frequency leads to the quick development of the liquefaction phenomenon and settlement and the liquefaction region was expanded. Fattah et al. [20] showed that the maximum settlement response of footing setting on dry sand samples is more than that on the fully saturated sand soil by about (5.0–10%). The maximum foundation displacement was reduced to a half value as the depth of the foundation was doubled for cases of dry and saturated sand.

The main goal of this research is to study the effect of using a subbase layer (sand cushion layer) under an embedded machine foundation at three frequencies ranging from low to high (w_r = 1000 and 2500 and 3500 rpm) on the liquefaction phenomena. Several parameters were considered in this study including:

a) The force time history of machine foundation.
b) The final settlement of the foundation.
c) The vertical stress inside the soil media under the machine's foundation.
d) The excess pore water pressure (EPWP) generated under the vibration load and the liquefaction evaluation.
e) The effect of subbase layer under footing required to reduce the liquefaction phenomena.

2. RESEARCH SIGNIFICANCE

This articulated research addressed an important phenomenon for sandy soil, which is the risk of liquefaction that increases during dynamic load on soil. The research introduced a scaled-down model of the liquefaction situation by imposing a vertical cyclic load. The finding is significant for understanding how liquefaction forms, especially while working in a sandy soil profile.

3. EXPERIMENTAL WORK

The methods include different stages, from the experimental setup to perform the tests.

3.1 Footing Model and soil properties

The properties of the steel footing with dimensions (300×200×50) mm are listed in Table 1. The physical and mechanical properties of the sand used in all models of footing are shown in Table 2.

3.2 Setup of Machine Foundation Model

The testing equipment and instrumentations are shown in Fig. 1 and Fig. 2. They consist of the following:

a) Machine-inducing vertical vibration.
b) Measurements of the Dynamic Response.
c) Steel container of dimensions (1000×800×600) mm.
d) Measurement of Dynamic force-time history (dynamic load cell).
e) Instruments to measure the settlement of footing by LVDT (Linear Variable Differential Transformer).
f) Instruments to calculate stresses in the soil medium using piezoelectric sensors.
g) Instruments to measure pore water pressure (PWP) by using pore water pressure transducers (PPT).

Table 2 Properties of steel footing

Item.	Property	Value
1	Secant modulus, GPa	37.4
2	Tangent modulus, GPa	140
3	Unit weight, kN/m^3	77

Table 1 Properties of the used sand

Soil Properties			Value	Standard
Specific Gravity, G_s			2.65	ASTM D854
Gravel (> 4.75 mm) %			0	
Sand (0.075-4.75 mm)%			97	
Silt and clay (< 0.075 mm)%			3	
Coefficient of curvature, C_c			1.55	
Coefficient of uniformity, C_u			1.73	
D_{10}, D_{30}, D_{60} (mm)			0.11, 0.18, 0.19	
Soil classification according to USCS			SP	ASTM D2487
Loose state relative density, RD %			24	
Medium state relative density, R_D %			50	
Dense state relative density, R_D %			75	
friction angle, ϕ	Loose state	Soaked	18.0	ASTM D3080
	Medium state	Soaked	32.0	
	Dense state	Soaked	39.0	
Permeability coefficient, k, (m/s)	Loose state		0.04	ASTM D2434-68
	Medium state		0.009	
	Dense state		0.005	

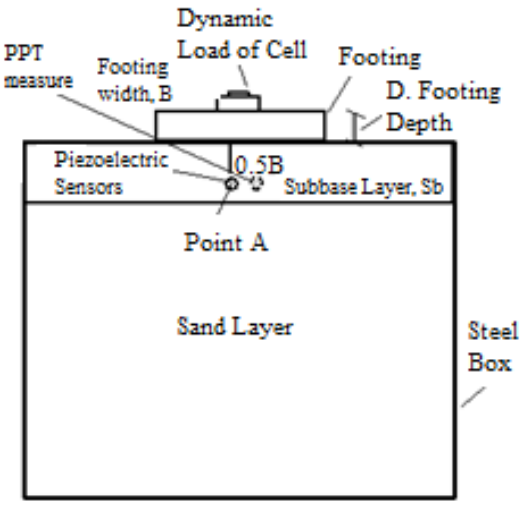

Fig. 1 Schematic diagram of the model and instrumentations

Fig 2 Photograph of the setup of sand model

3.3 Preparation and Placement of Models

The following procedures were adopted for the model preparation:

a) The internal faces of the steel box were covered with cork sheets. Such material acts as a damping boundary that can absorb the reflected waves.
b) The raining technique was used to pour the sand inside the steel box. The relative density of sand is proportional to the height that the sand particles will fall. Thus, several attempts were conducted to assess the falling height required for each relative density. Such procedures were obtained by Al-Jebouri [21].
c) The piezoelectric sensors and pore water pressure transducers were inserted at a depth 0.5 B under the footing base in order to read the stresses and pore pressure at this point. Continuous pouring of sand was done thereafter until it reached the specified level.
d) The top surface of the sand was leveled, and a perforated plate was placed at that surface. The water was added through this plate to
e) Ensure a uniform distribution of water all over the area until the sand is fully saturated.
f) The steel footing was placed at the center of the sand bed surface and the dynamic load cell was located at the footing center to record the dynamic load–time history.
g) The LVDT (Linear Variable Differential Transformer) was inserted at the edge of the footing to record the vertical settlement.
h) The above steps from (a-g) were repeated for each model test in order to achieve the relative density of model.

3.4 Testing Procedure

The footing was subjected to a vertical vibration load once the model preparation was completed. Mechanical oscillators with varying frequencies and eccentric settings were used to mimic various dynamic load levels in the vertical vibration testing. The amplitude of a dynamic force is proportional to the frequency at which it occurs.

Several parametric studies were adopted including the relative density of subbase layer (sand cushion) under the footing (R_D= 24%, 50%, 75%), the thickness of the subbase layer (D, and 1.5D), and the operating frequency of the mechanical oscillator (1000, 2500, 3500) rpm. The liquefaction potential was evaluated and the experimental results were plotted. The testing program of the experimental work is illustrated in Table 3.

Table 3 Parametric study

Model	Parameters			
	w_r, rpm	R_D %	Coefficient of permeability, k, m/sec	Thickness of subbase layer
Model-1	1000	24	0.04	D and 1.5D
Model-2	2500	24	0.04	
Model-3	3500	24	0.04	
Model-4	1000	50	0.009	
Model-5	2500	50	0.009	
Model-6	3500	50	0.009	
Model-7	1000	75	0.005	
Model-8	2500	75	0.005	
Model-9	3500	75	0.005	

4. RESULTS AND DISCUSSION

4.1 Force Time History

Fig. 3 shows the force time history which was recorded by a dynamic cell fixed at the middle of the footing at different frequencies of the machine and changed the state of soil from (loose to medium and dense state). The results show that the shape of load–time history coincides with the sine wave and the increase in the operating frequency lead to an increase in measured vibration load on the footing.

The maximum force recorded with changing the operating frequency which applies on the footing is illustrated in Fig. 4.

It is obvious that increasing the operating frequency from (1000 to 3500 rpm) leads to increase the maximum force from 5 N to 35 N, i.e. the increase is about 7 times.

Eq. (1) governed the shape of loads measured as below:

$$F_t = F_0 \sin w_t \quad (1)$$

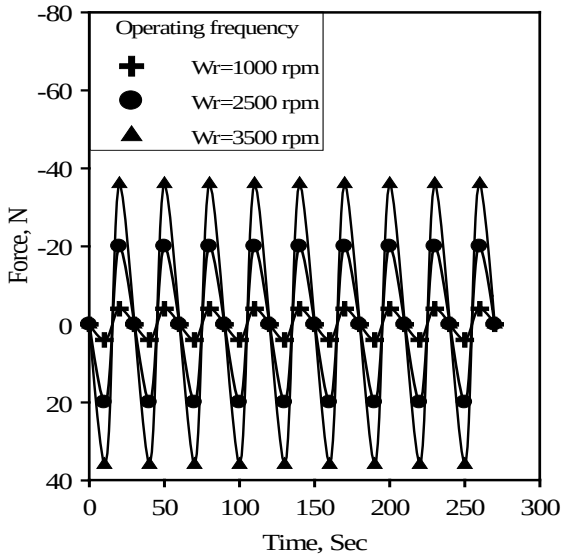

Fig. 3 Force - time history at a different operating frequency

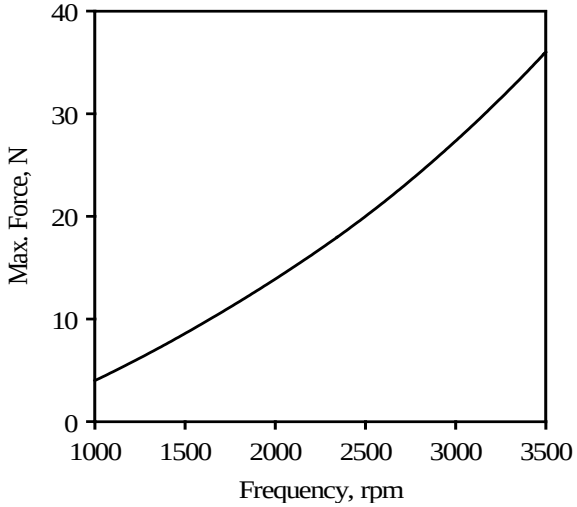

Fig. 4 Maximum force - time history with different operating frequencies

4.2 The Settlement of Machine Foundation

The effect of changing the operating frequency on the maximum settlement of footing resting on sand with different relative densities is shown in Fig. 5.

The results show that the settlement increases with increasing the operating frequency and decreases with increasing the relative density. A slight increase in the settlement is shown at R_D=75%, while it is more pronounced as the relative density becomes lesser.

A significant increase in the settlement appeared for R_D=24% and 50% after the frequency passes 2500 rpm to reach 6 times that appear at the initial value of the operating frequency. Loose sand contains large voids which can easily compact and increase the settlement. Similar findings by Fattah et al. [18] illustrated that the value of foundation settlement increases with increasing load amplitude.

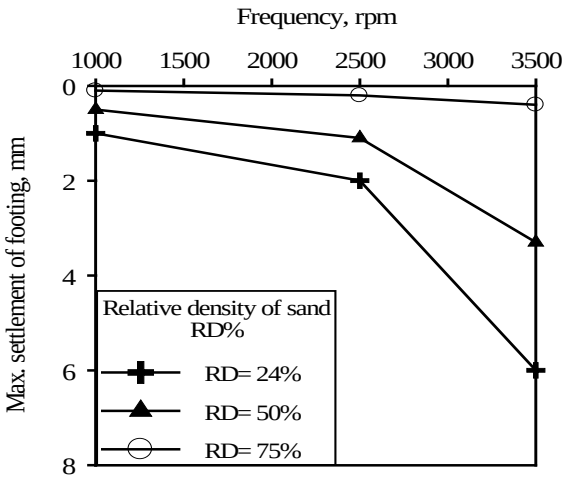

Fig. 5 Maximum settlement vs operating frequency at different relative densities

4.3 The Vertical Stress in Soil Media under Foundation

Fig. 6 illustrates the variation of vertical stress at point A, which is located at a depth of 0.5B below the footing base under different operating frequencies. The sand, at its dense state (R_D=75%) causes a good interlocking between the particles, which offers a wide area for the vertical stress to pass over the contact points.

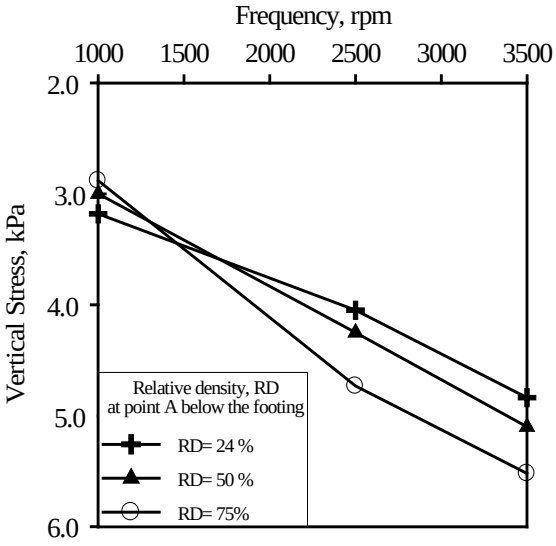

Fig. 6 Vertical stress in soil media with different operating frequencies

The vertical stress in the sand with R_D= 75% increases 3 times its initial value as the w_r increases from 1000 rpm to 3500 rpm compared to sand with R_D=24% and R_D=50% where the increase are about 1.5 times the initial values.

This is why the loose sand is considered a damping layer due to its low stiffness and the ability of such soil to dissipate energy through large voids. Seed et al. [22] mentioned that the value of soil material damping at small strains (strain < 10^{-5}) and the typical value ranged from 0.5% to 2% for sands. Since the material damping ratio is more dependent on the strain state, the material damping magnitude of sand soil can increase to 9% at a strain of 10^{-4}, and can exceed 20% at a strain of 10^{-3}.

4.4 The Excess of Pore Pressure under Foundation

The time history of excess pore pressure under the machine foundation at point A= 0.5B under the effect of different operating frequencies at different relative densities of sandy soil are depicted in Figs (7, 8, and 9). It is obvious that the maximum pore pressure value appeared at R_D=24% for w_r=3500 rpm, which represents 1.6 and 8 times that for R_D= 50% and 75%, respectively, which is applicable to Adalier and Elgamal [3].

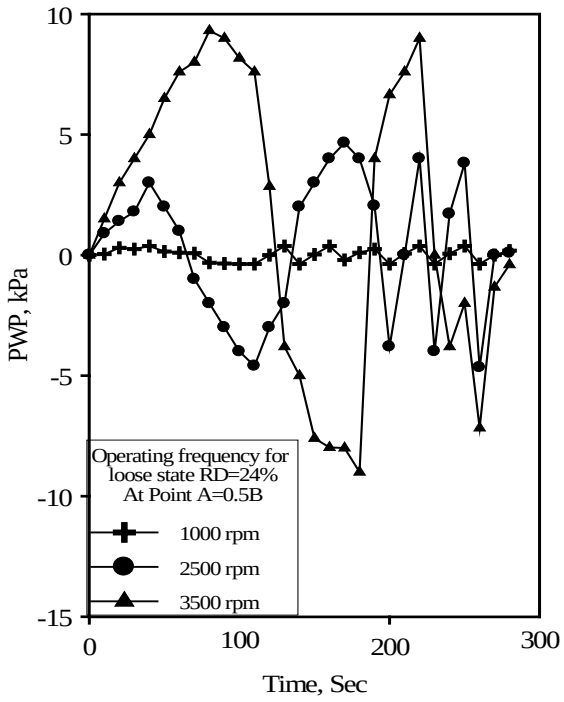

Fig. 7 Time history of pore pressure at the different operating frequencies, R_D=24%

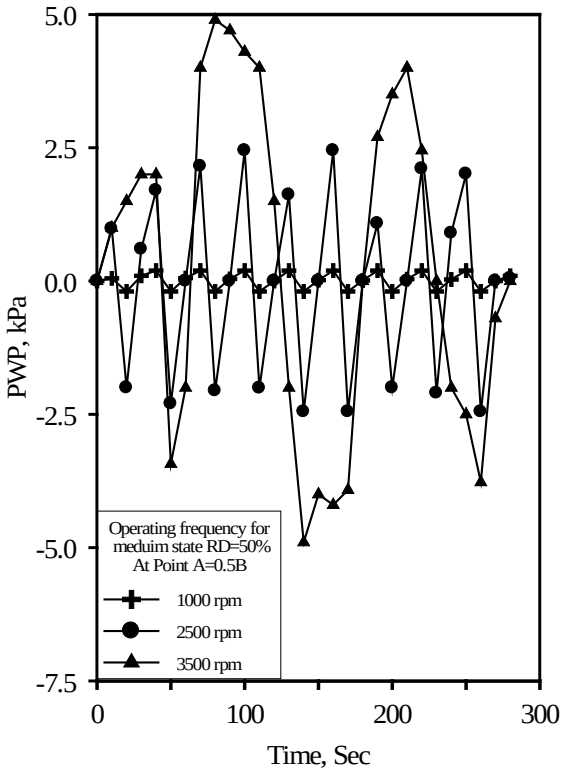

Fig. 8 Time history of pore pressure at different operating frequencies, R_D=50%

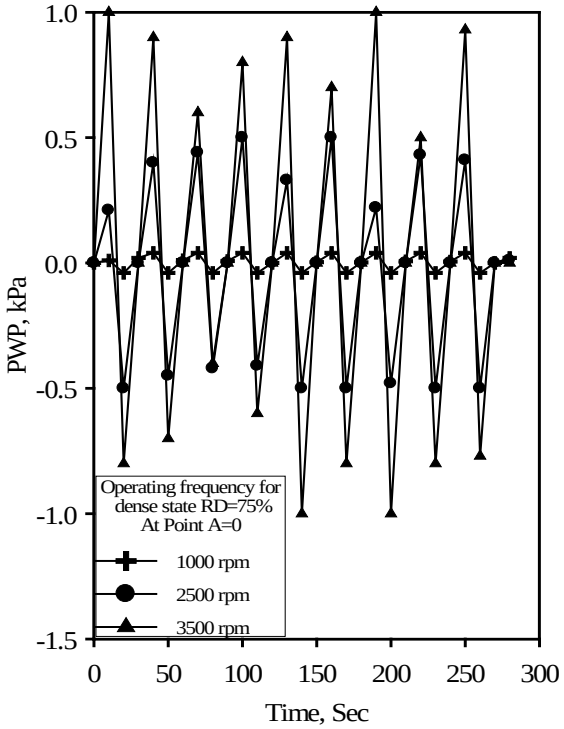

Fig. 9 Time history of pore pressure at different operating frequencies, R_D=75%

Large voids cause a higher pore pressure under the footing, especially at higher frequencies. An insignificant effect of pore water pressure is noticed at w_r= 1000 rpm through all the relative densities.

The value of pore pressure may be equal to or more than the vertical stress, especially at an operating frequency of more than (2500 rpm) which means the phenomenon of liquefaction will occur.

Figs 10, 11 and 12 show the results of the measured vertical stresses and pore pressure and the calculation of effective vertical stress by using the equations below:

$$\tau = c` + \sigma`_v \tan Ø` \quad (2)$$

$$\sigma` = \sigma - u \quad (3)$$

Where τ is the shear stress failure, c` is the cohesion, Ø` is the angle of internal friction, σ_v is the vertical stress, σ` is the effective vertical stress and u is the pore water pressure.

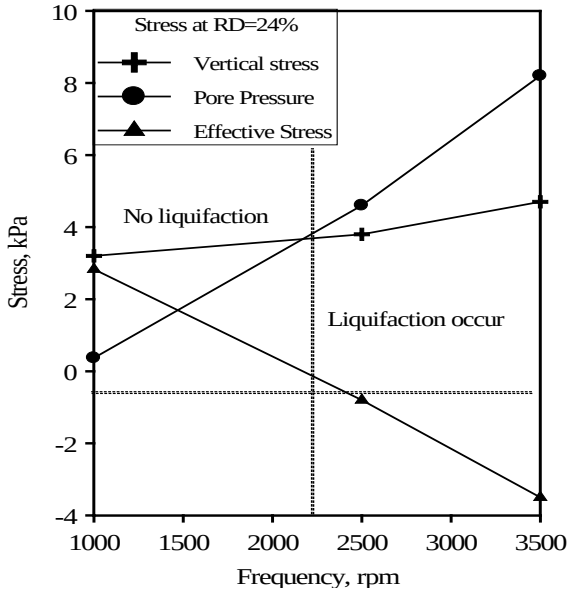

Fig. 10 Stress types with different operating frequencies at R_D=24%

It can be noticed from these figures that the effective stress becomes zero at a certain value of operating frequency, which means that the soil behaves as a liquid referring to the liquefaction phenomena. Fig 10 appears that the effective vertical stress for sand at a loose state (R_D=24%) becomes zero at w_r= 2200 rpm due to the pore water generation under the machine foundation. The sand needs a higher operating frequency to cause liquefaction phenomena with increasing relative density. The effective negative stress occurs when the excess pore pressure value becomes more than the value of vertical stress at which the soil behaves as a liquid. Such a case can be maintained if the applied dynamic load is continued under undrained conditions.

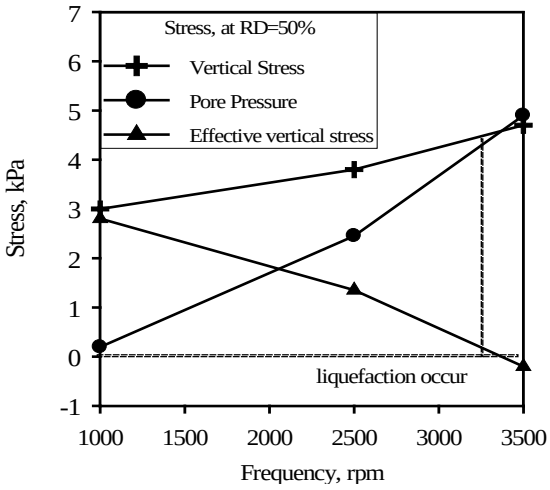

Fig. 11 Stress types with different operating frequencies at R_D=50%

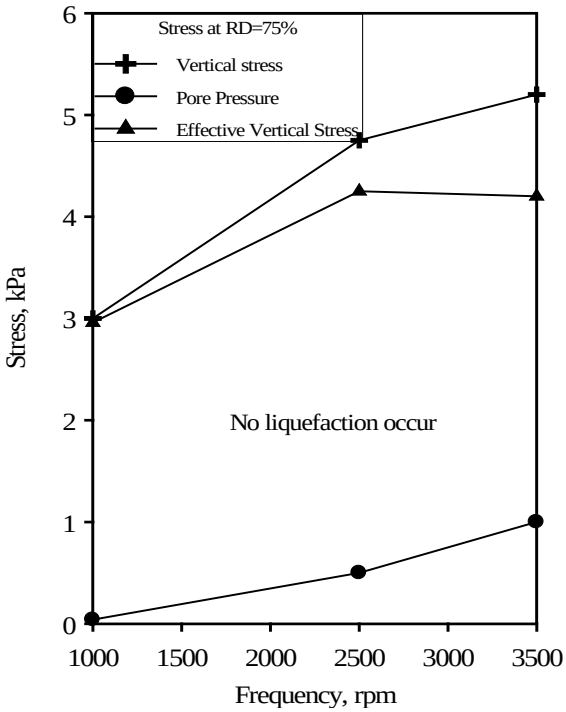

Fig. 12 Liquefaction of sandy soil and subbase layer during testing and PPT measurement

This is obvious in Fig. 11 where the effective vertical stress becomes zero at an operating frequency w_r=3350 rpm. No liquefaction is noticed in the dense sand (R_D=75%), as shown in Fig. 12, due to small voids at this state compared to the void ratio at the loose state. In other words, the value of

vertical stress generated in soil media and the state of the soil related to the volume of void ratio has a great impact on the mobilization of liquefaction phenomena. Fig. 13 shows the liquefaction phenomena which appeared during the test.

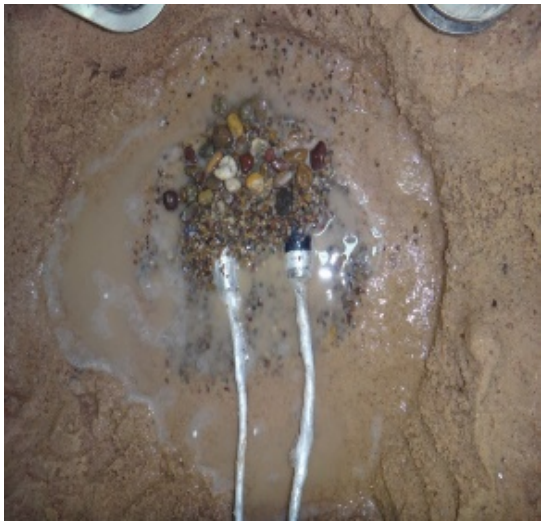

a)

b)

Fig. 13 Liquefaction of sandy soil and subbase layer during testing and PPT measurement

4.5 The Effect of Subbase Layer Thickness on Liquefaction

The impact of the thickness subbase layer type B according to the ASTM D1241-15 on the phenomena of liquefaction is illustrated in Figs. 14 and 15 when the sand is at a loose state (R_D= 24%). It can be seen that the subbase layer plays an important role in minimizing the liquefaction risk.

Fig. 14 shows that using a subbase layer with a thickness equal to the footing's depth (S_b = D) reduces the opportunity for liquefaction at a moderate value of operating frequency. Liquefaction appears at a higher operating frequency (greater than 3250 rpm) due to the generation of pore water pressure.

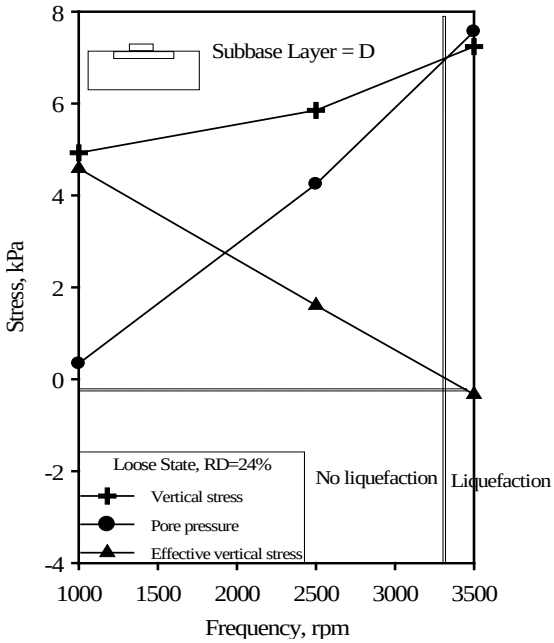

Fig. 14 Stress versus operating frequency at thickness = D of sub base

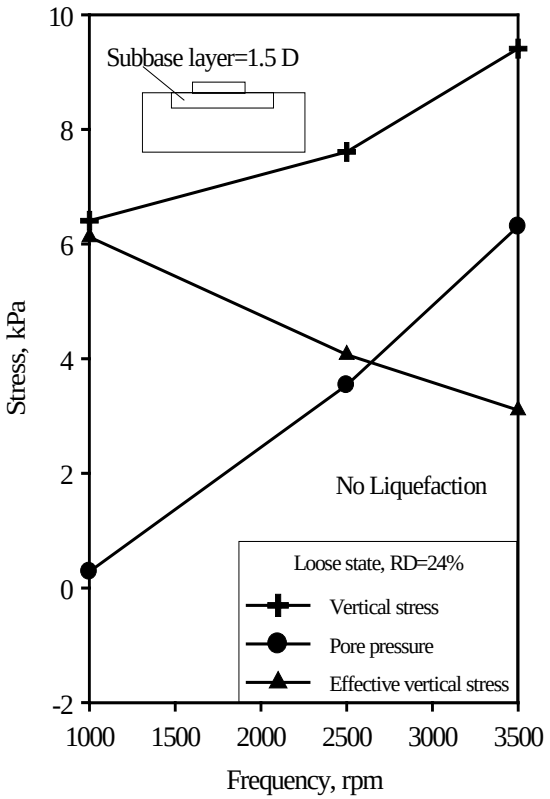

Fig.15 Stress versus operating frequency at a thickness of subbase layer = 1.5 D for RD=24%.

5 CONCLUSIONS

The following conclusions can be drawn from this study:

a) The shape of load–time history coincides with a sine wave and the increases in operating frequency led to increasing the measured vibration load on the footing. The maximum force increases to about 7 times with increasing the operating frequency (w_r) from 1000 to 3500 rpm.
b) A significant increase in the settlement appeared for R_D=24% and 50% after the frequency (w_r) passes 2500 rpm to reach 6 times that appears at the initial value of the operating frequency.
c) The vertical stress in the sand with R_D= 75% increases 3 times its initial value as the frequency (w_r) increases from 1000 rpm to 3500 rpm compared to sand with R_D=24% and R_D=50% where the increase is about 1.5 times the initial values.
d) Liquefaction appears when the sand is at its loose state (R_D=24%) and w_r=2100 rpm. At the medium state (R_D=50%) the phenomena of liquefaction need a higher operating frequency (w_r=3250 rpm).
e) Increasing the thickness of the subbase layer up to 1.5 D leads to an increase in the vertical stress through the soil media and decreases the excess pore pressure, which eliminates the effect of liquefaction.

6 ACKNOWLEDGMENTS

The authors would like to thank Mustansiriyah University, Baghdad, Iraq, for the support provided during the present work.

7 REFERENCES

[1] Dash SR, and Bhattacharya S., Por Water Pressure Generation and Dissipation Near to Pile and Far-Field in Liquefiable Soils, International Journal of GEOMAT, 2015, Vol. 9, Issue. 2, 2015, pp. 1454-1459

[2] Das B. M., and Ramana G., Principles of Soil Dynamics, 2nd Edition, Cl-Engineering, U.S.A., 2011, pp. 1-673.

[3] Adalier K., and Elgamal A., Liquefaction of over-consolidated sand: A centrifuge investigation. Journal of Earthquake Engineering, Vol. 9, Issue 1, 2005, pp. 127–150.

[4] Al-Azawi T. K., Al-Azawi R. K., and Al-Jaberi Z. K., Stiffness and Damping Properties of Embedded Machine Foundation. Journal of Engineering, Vol. 12, Issue 2, 2006, pp. 429-443.

[5] Chandrakaran S., Vijayan P. and Ganesan N., A Simplified Procedure for Design of Machine Foundations Subjected to Vertical Vibrations, Journal of the Institution of Engineers. India. Civil Engineering Division, Vol.88, Issue 5, 2007, pp. 3-12.

[6] Jafarzadeh F. and Asadinik A., Dynamic Response and Impendence Functions of Foundation Resting on Sandy Soil Using Physical Model Tests, The 14 World Conference on Earthquake Engineering, 2008, Beijing, China.

[7] Vivek P., and Gosh, P., Dynamic Interaction of Two nearby Machine Foundation on Homogeneous Soil, Geo-Congress, 2012, pp. 21-30.

[8] Al-Shammary W. T. S., Numerical Analysis of Machine Foundation on Saturated Sandy Soil, M.Sc. Thesis, Building and Construction Engineering Department, University of Technology, Iraq, 2013.

[9] Swain A., and Ghosh P., Experimental Study on Dynamic Interference Effect of Two Closely Spaced Machine Foundations, Canadian Geotechnical Journal, Vol. 53, Issue 2, 2016, pp. 196–209.

[10] Keawsawasvong S., Senjuntichai T., Plangmal R., and W. Kaewjuea W., Rocking Vibrations of Rigid Foundations on Multi-Layered Poroelastic Media, Marine Georesources and Geotechnology, Vol.38, Issue 4, 2020, pp. 480-492.

[11] Hassan F., and Salwan A., Dynamic Response of Machine Foundation Resting on Sand-Granulated Tire Rubber Mixtures, MATEC Web Conferences. Vol. 162, 2018.

[12] Tileylioglu S., Stewart J. P., and Nigbor R., Dynamic Stiffness and Damping of a Shallow Foundation from Forced Vibration of a Field Test Structure, Journal of Geotechnical and Geoenvironmental Engineering, Vol. 137, Issue 4, 2010, pp. 344-353.

[13] Alzabeebee S., Dynamic response and design of a skirted strip foundation subjected to vertical vibration, Geomechanics and Engineering, Vol. 20, Issue 4, 2020, pp. 345–358.

[14] Fattah M.Y., Al-Neami M.A., Jajjawi N.H., Prediction of liquefaction potential and pore water pressure beneath machine foundations, Central European Journal of Engineering Vol. 4, Issue 3, 2014, pp. 226-249.

[15] Javdanian H., Behavioral interference of vibrating machines foundations constructed on sandy soils, International Journal of Engineering, Transactions B: Applications, Vol. 31, Issue 4, 2018, pp. 548–553.

[16] Choudhury D, Rao K.S.S, (2005) Seismic bearing capacity of shallow strip footings,

Journal of Geotechnical and Geological Engineering, Vol. 23, 2005, pp. 403–418.

[17] Bhatia K., Foundations for Industrial Machines: Handbook for Practicing Engineers, 1st Edition, D-CAD Publishers, New Delhi, 2008, pp. 1-675.

[18] Fattah M. Y., Salim, N. M., Haleel, R. J., Liquefaction Potential of Sandy Soil from Small Laboratory Machine Foundation Model, International Review of Civil Engineering (I.RE.C.E.), Vol. 9, Issue 1, 2018, pp. 11-19.

[19] Fattah M. Y., Al-Neami M. A., Jajjawi N. H., Prediction of Liquefaction Potential and Pore Water Pressure beneath Machine Foundations, Central European Journal of Engineering, Vol. 4, Issue 3, 2014, pp. 226-249.

[20] Fattah M. Y., Al-Mosawi M. J., Al-Ameri, A. F. I., Dynamic Response of Saturated Soil – Foundation System Acted upon by Vibration, Journal of Earthquake Engineering, Taylor & Francis Group.Vol. 21, Issue 7, 2017, pp. 1158-1188.

[21] Al-Jebouri J.M., Bearing Capacity of Footing on Reinforced Sand, M.Sc. Thesis, University of Baghdad, Iraq, 1986.

[22] Seed H.B., Wong R.T., Idriss IM, and Tokimatsu, K., Moduli and Damping Factors for Dynamic Analyses of Cohesionless Soils, Journal of Geotechnical Engineering, Vol. 112, Issue 11, 1986, pp. 1016-1032.

[23] Al-Soud M.S., Fartosy S.H., Jabur A.R., Majeed, M.W., Madhloom, H.M., and Al-Ansari N., Sustainable Improvement of Bentonite Clay Characteristics by Adding Pulverized Waste Glass, International Journal of GEOMATE, Vol. 23, Issue 95, 2022, pp. 10–19.